Journal of Biomolecular NMR, 6 (1995) 313–320
ESCOM

J-Bio NMR 297

Parametrisation of time-averaged distance restraints in MD simulations

Alain P. Nanzer, Wilfred F. van Gunsteren* and Andrew E. Torda**

Department of Physical Chemistry, ETH Zentrum, CH-8092 Zürich, Switzerland

Received 19 April 1995
Accepted 14 July 1995

Keywords: Time-averaged distance restraints; Parametrisation; MD simulation

Summary

Time-averaged restraints in molecular dynamics simulations offer a means to account for the averaging that is implicit in NMR spectroscopic data. We present a systematic investigation of the parameters which characterise time-averaged distance restraints. Using previously published data for a small protein, chymotrypsin inhibitor 2, we identify conditions which can lead to undesirable heating or which grossly distort the dynamics of the system.

Introduction

The refinement of structures from X-ray crystallography (Blundell and Johnson, 1976) or multidimensional NMR spectroscopy (Wüthrich, 1986) is a lively area of computational chemical methodology. Complementing distance geometry, molecular dynamics (MD) simulations play an essential role in the final phase of refining high-resolution structures of biomolecules. In MD refinement using NMR data, ^{3}J-coupling constant restraints and NOE distance restraints are used in two separate artificial potential energy functions that restrain the structure so as to satisfy the experimental input data during the simulation. Unfortunately, such potential energy functions usually model the solution structure as a single conformation, with little concession to the fact that NMR measurements really reflect a time average (Jardetzky, 1980).

One approach to accounting for these dynamic effects has been the development of pseudo-potential energy functions, which only try to coerce an average property to agree with the experimental data (Torda et al., 1989, 1990,1993). This work, along with later studies (Pearlman and Kollman, 1991; Schmitz et al., 1992,1993; Nanzer et al., 1994; Pearlman, 1994a,b) has demonstrated the ability of this technique to sample a larger conformational space and – at the same time – satisfy the experimental data. This work also served to highlight the importance of analysing whole MD trajectories, rather than the single structures which are the end points of MD refinement trajectories.

Time-averaged distance restraints are characterised by two parameters, i.e., the force constant K_{dr}, which determines the strength of the additional restraining force, and τ_{dr}, which is the length of the memory decay time to average the distances during the simulation. These parameters have been investigated by several authors under different conditions and with different macromolecules. The first such calculation was done on the 74-residue protein Tendamistat, where two different force constants K_{dr} (15 and 25 kJ mol^{-1} Å^{-2}) and two small memory decay times τ_{dr} (0.5 and 1.25 ps) were used (Torda et al., 1990). The parameters were used without any systematic investigation. A similar calculation, based on a DNA oligomer, was described shortly afterwards. These authors used synthetic data, varied the force constant K_{dr} and applied a fixed decay time $\tau_{dr}=20$ ps (Pearlman and Kollman, 1991). Schmitz et al. (1993) did the same, but with real data. In 1994, Pearlman published an investigation of parameters and effects of time-averaged distance restraints, again using synthetic data from a cyclic peptide (Pearlman, 1994a). Different force constants K_{dr} (0.5 to 8 kJ mol^{-1} Å^{-2}) and a fixed memory decay time τ_{dr} (20 ps) were applied. Similar work on time-averaged ^{3}J-coupling constant restraints was later presented by the same author (Pearlman, 1994b).

In the present paper we try to give some further in-

*To whom correspondence should be addressed.
**Present address: Research School of Chemistry, Australian National University, Canberra 0200, Australia
Abbreviations: NOE, nuclear Overhauser effect; MD, molecular dynamics; CI-2, chymotrypsin inhibitor 2.

sights into the effects of time-averaged restraints in MD simulations on a known protein structure. Pearlman (1994a,b) used unrestrained MD trajectories as the source of the 'experimental' data. This provides the comfort of an exact force field and precise distance restraints. The advantage of our approach is the fact that real data bring along a set of real problems, such as lack of precision, uneven distribution of data over the molecule and the possibility that minima in the force field will not coincide with minima with respect to the experimental data. One may also note that these flaws are, unfortunately, not quantified. This suggests a series of questions. Which parameter sets allow one to refine a structure of a protein? Can we make better statements about the dynamics of the simulated molecule with optimal combinations of parameters? Furthermore, the influence of the length of the decay time τ_{dr} has not been investigated in a systematic way. Again, several questions can be formulated. Does the length of τ_{dr} disturb the dynamics of the system or are we really simulating the natural dynamics of the protein? The additional non-conservative restraining potential energy function can increase the kinetic energy of the simulated system (Pearlman, 1994b). Is it possible to avoid this effect by choosing a longer decay time τ_{dr}?

The calculations presented here were performed on the 64-residue structured domain of chymotrypsin inhibitor 2 (CI-2), for which refined solution structures have been published (Clore et al., 1987; Ludvigsen et al., 1991a,b; Nanzer et al., 1994). The values of the relevant parameters were spread over a wide range, so as to see effects of extreme values. The force constant K_{dr} was varied from 1 to 100 kJ mol^{-1} Å^{-2} and the memory decay time τ_{dr} was varied from 2 to 50 ps.

Methods

Theory

Molecular dynamics simulations are usually employed for the refinement of NMR-based structures by constructing an artificial energy term that raises the energy of the system as violations of the experimental data increase (van Gunsteren et al., 1984; Kaptein et al., 1985). In the GROMOS force field (van Gunsteren and Berendsen, 1987), this term is quadratic with respect to violations of distance constraints, so that:

$$V_{dr}(r) = \begin{cases} \frac{1}{2}K_{dr}(r - r_0)^2 & \text{if } r > r_0 \\ 0 & \text{if } r \le r_0 \end{cases} \quad (1)$$

where $V_{dr}(r)$ is the potential energy due to the distance restraint term for a given pair of atoms, r is the instantaneous distance between the cross-relaxing nuclei and r_0 is the distance calculated from the measured NOE. A force constant, K_{dr}, is used to weigh this term relative to the rest of the force field.

For time-averaged distance restraints we used a force introduced by Torda et al. (1990), where:

$$\vec{F}_i(t) = \begin{cases} -K_{dr}(\bar{r}_{ij}(t) - r_0)\dfrac{\vec{r}_{ij}(t)}{r_{ij}(t)} & \text{if } \bar{r}_{ij}(t) > r_0 \\ 0 & \text{if } \bar{r}_{ij}(t) \le r_0 \end{cases} \quad (2)$$

Here $\vec{F}_i(t)$ is the force on atom i due to atom j at time t, $\vec{r}_{ij} = \vec{r}_i - \vec{r}_j$ and $\bar{r}_{ij}(t)$ is the time-averaged distance between atoms i and j. $\bar{r}_{ij}(t)$ is calculated using an exponentially decaying weight factor

$$\bar{r}(t) = \left(\frac{1}{\tau_{dr}\left(1 - e^{-t/\tau_{dr}}\right)} \int_0^t e^{-t'/\tau_{dr}} \left[r(t - t')\right]^{-3} dt' \right)^{-1/3} \quad (3)$$

where τ_{dr} is the characteristic time for the exponential decay. Integration of Eq. 2 with respect to the instantaneous distance would lead to some expression for the instantaneous potential energy, but the time averaging inherent to this term makes the potential energy lose its normal physical meaning. Effectively, this force field term is no longer conservative and it would be inappropriate to treat it as such. For this reason, we do not refer to a restraint energy. Equation 3 is based on averaging r^{-3} distances. This is appropriate for simulations that are too short to properly average over angular fluctuations (Tropp, 1980).

For each measured ^{3}J-value, a restraining potential V_J was calculated so as to directly restrain the coupling constant rather than the calculated dihedral angle. Time-averaged restraints were imposed according to Eq. 4 (Torda et al., 1993):

$$V_J = \tfrac{1}{2}K_J\left(\bar{J}(\theta(t)) - J_0\right)^2 \quad (4)$$

where $J(\theta)$ is the coupling constant calculated from the dihedral angle θ, J_0 is the measured value, K_J is a force constant and $\bar{J}(\theta(t))$ is the time-averaged coupling constant, calculated according to Eq. 5:

$$\bar{J}(\theta(t)) = \frac{1}{\tau_J\left(1 - e^{-t/\tau_J}\right)} \int_0^t e^{-t'/\tau_J} J(\theta(t - t'))\,dt' \quad (5)$$

Again, τ_J is the characteristic time for the exponential decay. Note that, as in our previous work, we assume that $t \gg \tau$, so that:

$$1 - e^{-t/\tau} \approx 1 \quad (6)$$

and this factor is dropped from both Eqs. 3 and 5.

Molecular model and simulation setup

All simulations were carried out using software from the GROMOS suite of programs and the GROMOS

TABLE 1
AGREEMENT WITH EXPERIMENTAL DATA AS A FUNCTION OF SIMULATION PARAMETERS

K_{dr} (kJ mol^{-1} Å^{-2})	τ (ps)	$E_{POT-TOT}$ (kJ mol^{-1})	Sum of violations (Å)	Largest violation (Å)	Temperature (K)
1	0	−1169±98	120	3.38	296.5±8.2
	2	−1096±67	139	3.15	297.9±8.2
	5	−1194±73	137	3.88	297.1±8.1
	10	−1199±70	184	4.47	296.9±8.2
	20	−1161±73	162	4.10	296.7±8.1
	50	−1230±83	200	3.94	296.6±8.1
3	0	−978±68	63	1.87	296.4±8.2
	2	−962±77	87	2.09	299.4±8.3
	5	−994±81	91	2.94	297.9±8.2
	10	−1028±72	94	2.47	297.3±8.2
	20	−1078±72	101	2.79	296.9±8.2
	50	−1084±93	121	2.47	296.7±8.2
10	0	−754±70	33	0.76	296.4±8.1
	2	−668±78	46	1.31	302.8±8.5
	5	−712±85	47	1.37	299.5±8.3
	10	−766±80	51	1.26	298.2±8.2
	20	−833±93	57	1.32	297.4±8.2
	50	−905±102	65	1.66	296.9±8.2
30	0	−351±70	19	0.89	296.2±8.2
	2	163±127	26	0.80	323.5±12.0
	5	−374±101	33	0.83	303.2±8.6
	10	−448±107	35	0.83	300.2±8.3
	20	−496±134	37	0.76	298.6±8.3
	50	−606±157	45	1.13	297.5±8.2
60	0	−70±57	11	0.63	296.2±8.2
	2	180±129	29	0.77	324.8±11.6
	5	12±127	29	0.66	308.9±9.3
	10	−87±147	30	0.64	303.2±8.7
	20	−179±162	32	0.75	300.0±8.4
	50	−309±212	40	0.96	297.5±8.2
100	0	290±63	7	0.54	296.1±8.3
	2	590±146	26	0.74	338.2±14.3
	5	444±170	29	0.67	316.3±10.7
	10	283±178	30	0.64	306.9±9.1
	20	190±234	33	0.83	302.3±8.5
	50	−3±298	38	1.14	299.0±8.3

K_{dr} and τ_{dr} are the force constant and memory decay constant used for distance restraints. All values are averages calculated over 0.5 ns trajectories. The average total potential energy, including the distance restraints energy, and the temperature are quoted ± the rms fluctuation over the trajectory.

37D4 united atom force field for in vacuo simulations (van Gunsteren and Berendsen, 1987). The temperature was held constant by weak coupling ($\tau_T = 0.1$ ps) to an external bath of 300 K (Berendsen et al., 1984). The SHAKE algorithm was used to maintain all bond lengths with a relative precision of 10^{-4} (Ryckaert et al., 1977) and the integrator time step was 0.002 ps.

The set of 961 distance restraints and 39 J-coupling constant restraints is the same as used by Nanzer et al. (1994) and has been given by Ludvigsen et al. (1991b). Pseudo and virtual atoms for distance restraining were defined as in Wüthrich et al. (1983), van Gunsteren et al. (1985) and van Gunsteren and Berendsen (1987). Simulations with time-averaged distance restraints require the choice of an initial value $\bar{r}(0)$. For all the runs using time-averaged distance restraints, $\bar{r}(0)$ was set, for each distance restraint, to 0.2 Å less than r_0.

Our single starting structure has also been used by Nanzer et al. (1994). This was a previously published structure (Ludvigsen et al., 1991b) that was subjected to 1000 steps of energy minimisation, followed by simulations of 10 and 20 ps, using $K_{dr} = 20$ kJ mol^{-1} Å^{-2}, $K_J = 20$ kJ mol^{-1} s^2 and $\tau_{dr} = \tau_J = 0$ ps, that were performed to equilibrate the system in the GROMOS force field. The obtained structure was then used as the starting point for a series of 0.5 ns MD simulations. In this series of simulations, τ_{dr} varied from 0 to 50 ps and K_{dr} from 1 to 100 kJ mol^{-1} Å^{-2}, as detailed in Table 1.

Results

Two parameters characterise time-averaged MD simulations, i.e., the force constant K_{dr} and the length of the decay constant for the memory, τ_{dr}. The force constant K_{dr} controls the relative weight of the artificial restraining term in the force field. τ_{dr} determines the length of the exponential decay in Eq. 3 and the system's sensitivity to history. Table 1 summarises a series of 0.5 ns simulations in which the two parameters were systematically varied. Quantities reflecting agreement with experimental data and energetic properties are discussed below. For the analysis, average properties were calculated without a memory function ($\tau_{dr} = \tau_J = \infty$), since the average over the whole simulation trajectory must agree with the experimental data.

Agreement with experimental data

As in our previous MD simulations of this system (Nanzer et al., 1994), all 39 measured ^{3}J-coupling constants were accurately reproduced. Because our main focus is the investigation of different distance restraining force constants K_{dr} and the appropriate memory decay constant τ_{dr}, we concentrate our discussion on the effects of the 961 distance restraints.

Agreement with experimental restraints was judged by two criteria, as shown in Table 1. We quote firstly the sum of distance restraint violations, and secondly the largest single violation, as this is indicative of possible problems with the structure and is independent of the number of restraints.

Simulations using force constants K_{dr} smaller than 10 kJ mol^{-1} Å^{-2} (see Table 1 and Fig. 1) all show an increased sum of violations compared to that of the relaxed starting structures (sum of violations of 40 Å). In contrast, force constants K_{dr} larger than 10 kJ mol^{-1} Å^{-2} always reduce

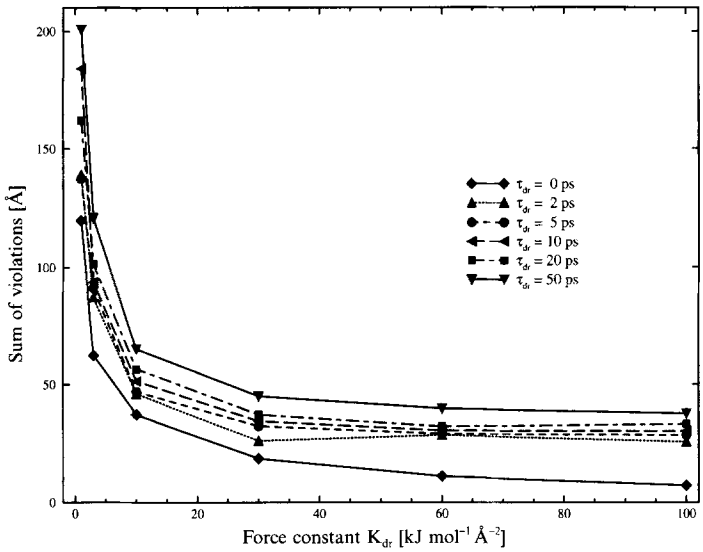

Fig. 1. Sum of violations for the 961 upper distance restraints for all simulations of CI-2, using different parameter sets. All values are trajectory averages.

the sum of violations. The smallest sum, 7 Å, is reached without time averaging and with the highest force constant K_{dr}. This also leads to the smallest 'largest violation' of 0.54 Å. The 'largest violations' cover quite a wide range, from 0.5 to 4.5 Å, and indicate that not all combinations of K_{dr} and τ_{dr} yield reasonable agreement with the experimental data. Figure 1 summarises the influence of the parameters on the sum of violations. Choosing a larger force constant significantly reduces the sum of violations during the MD simulation. Surprisingly, τ_{dr} has little effect on the agreement with experimental data. Its influence on the dynamics of the system is discussed below.

In the extreme case of $\tau_{dr}=0$ ps (instantaneous restraints), there is a slight reduction in the sum of violations, as seen in previous simulations of this system (Nanzer et al., 1994). This is in contrast to earlier results on comparable systems (Torda et al., 1990; Pearlman and Kollman, 1991). There are several possible reasons for this behaviour. If the experimental data really are not influenced by the dynamics of the molecule, then a static model of the structure and a time-averaged model should agree equally well with the data. In practice, the time-averaged restraints will allow the system to temporarily violate the restraints, which might result in small, but systematic, violations. It is unlikely that any data set will be totally immune to the influence of motions, but this is a matter of degree.

Energetic behaviour of restrained MD simulations

From Table 1, it can be seen that the average potential energy of the system at about 300 K spans a range from −1230 to 590 kJ mol^{-1}. The fluctuation of the potential energy reflects the dynamic behaviour of the structure during an MD simulation. Not surprisingly, the values diverge greatly for the different combinations of parameters. Root-mean-square (rms) fluctuations ranging from 57 to 298 kJ mol^{-1} were obtained for the different simulations.

Comparing the results with the total potential energy calculated for the initial 30 ps equilibration simulation ($E_{POT\text{-}TOT}=89.6$ kJ mol^{-1}, its fluctuation 96.6 kJ mol^{-1}), it is again possible to arbitrarily divide the results into two groups, containing results better or worse than the equilibration simulation. Simulations using force constants $K_{dr}=10$ kJ mol^{-1} Å^{-2} or less result in a lower potential energy, independent of the value of τ_{dr}. Force constants $K_{dr}=30$ or 60 kJ mol^{-1} Å^{-2} result in a more favourable energy, except for $\tau_{dr}=2$ ps. When $K_{dr}=100$ kJ mol^{-1} Å^{-2} all possible τ_{dr} values, except $\tau_{dr}=50$ ps, yield higher energies.

Figure 2 summarises the effects of different parameter combinations and clearly shows the dominant influence of the force constant K_{dr}: the higher the force constant, the more energy the restraining penalty function adds to the total potential energy. It can be seen that increasing τ_{dr} generally results in lower energies, but turning off the time averaging ($\tau_{dr}=0.0$ ps) results in a lower potential energy than using a small τ_{dr}.

Table 1 shows that fluctuations of the potential energy increase as the average potential energy increases. Force constants K_{dr} equal to or smaller than 10 kJ mol^{-1} Å^{-2} do not have much effect on the fluctuations, regardless of the value of τ_{dr}. Significantly larger fluctuations were seen with larger force constants K_{dr} and time-averaging periods (τ_{dr}) longer than 5 ps.

The comparison of total potential energies shows that time-averaged distance restraints increase the energy of the molecule, especially when using large force constants and short τ_{dr} values. Two important questions arise from these results. First, does the additional penalty function

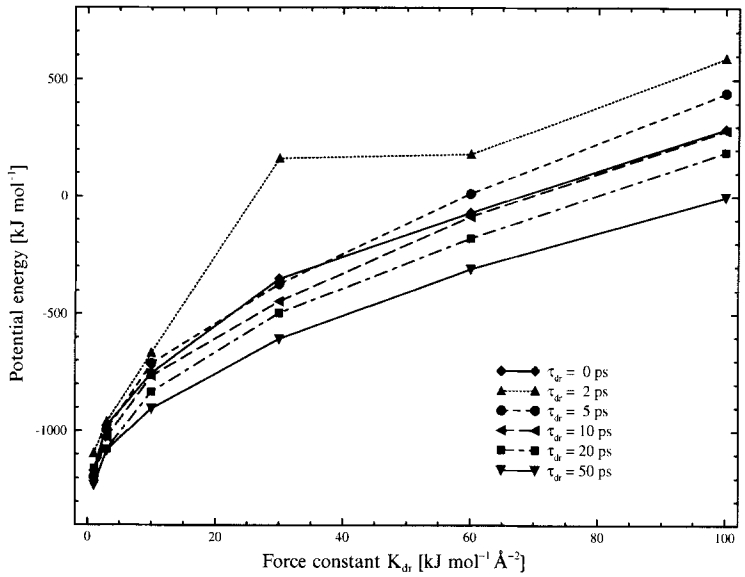

Fig. 2. Molecular potential energy, including distance restraints energy, for C1-2 for all parameter sets. All values are trajectory averages.

for the distance restraints increase the temperature of the whole system or of just a part, and second, if higher temperatures occur, which parts of the molecules suffer from this additional energy?

Table 1 also lists the average temperatures and their fluctuations. In all simulations where the force constant K_{dr} is smaller than 30 kJ mol^{-1} Å^{-2}, hardly any effect on the temperature is observed. Using force constants K_{dr} equal to or greater than 30 kJ mol^{-1} Å^{-2}, the average temperatures are increased for small τ_{dr}. The combination of a small τ_{dr} with large force constants K_{dr} heats the system. The temperature increase for large force constants K_{dr} can be avoided by using longer τ_{dr} values. This effect can be seen very clearly in Fig. 3, where the temperatures are plotted against the force constants K_{dr}. As the temperature increases, the temperature fluctuations also increase, see Table 1.

As has been noted previously (Torda et al., 1990; Pearlman, 1994a), the use of time-averaged restraints may sometimes cause heating of the system and this heating will not be evenly distributed over the molecule. We attempted to investigate this phenomenon in more detail. Although the concept of temperature does not have a meaning when applied to single atoms, we did calculate the square of the velocity $\vec{v}_i$ for each atom i, multiplied by the mass m_i and divided by three times Boltzmann's constant k, which we can refer to as a temperature for convenience. For each residue, we then averaged this temperature separately over the backbone atoms and over the side-chain atoms. The upper half of Fig. 4 shows the

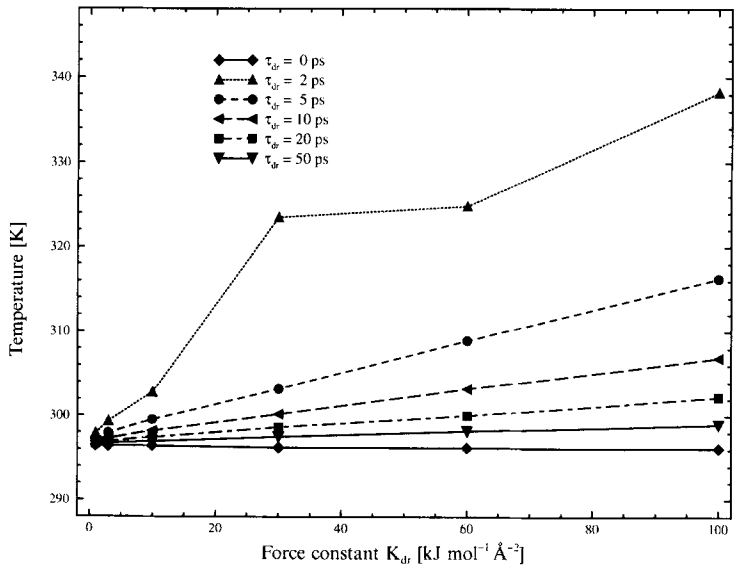

Fig. 3. Temperature for all simulations using different parameter sets. All values are trajectory averages.

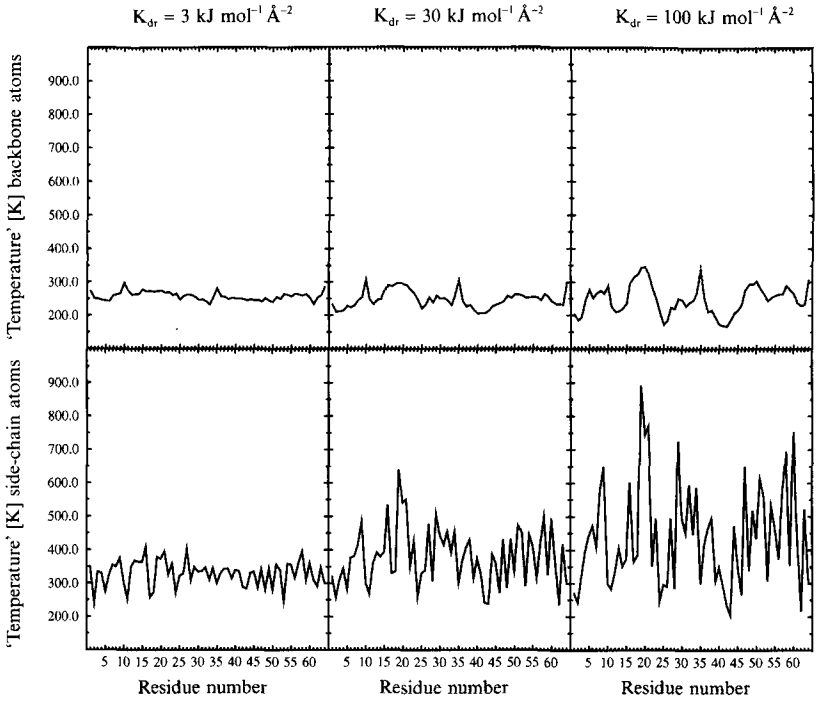

Fig. 4. 'Temperature' defined as explained in the text for selected atom groups of CI-2, plotted versus their residue number. The upper panels show the temperature for the backbone atoms of CI-2, applying a memory decay time $\tau_{dr} = 2$ ps and force constants $K_{dr} = 3$, 30 and 100 kJ mol^{-1} Å^{-2} (from left to right). The lower panels show the same, but for the side-chain atoms of each residue.

temperatures of the backbone atoms for each residue with force constants $K_{dr} = 3$, 30 and 100 kJ mol^{-1} Å^{-2} and $\tau_{dr} =$ 2 ps. The lower half shows the corresponding quantities for side-chain atoms. The differences are obvious; whereas the temperature of the backbone is hardly increased, the temperature of the side-chain atoms varies as a function of residue up to three times more than for the backbone atoms. Furthermore, the heating depends on the value of K_{dr}. Clearly, the side-chain atoms are subject to artificial heating.

Heating of the system is undesirable, but only occurs for particular combinations of values of the simulation parameters. What is more disturbing is the possibility that the worst effects of this heating may be masked by the temperature bath. All the simulations were performed using weak coupling to a temperature bath (Berendsen et al., 1984), where the temperature is calculated over the whole system and all velocities are scaled uniformly. This may well lead to a situation where part of the molecule is heated by the artificial forces, and the whole molecule is cooled by the temperature coupling mechanism. This means that what appears to be a system at equilibrium is actually a system in a steady state, with a constant heat flow away from the hot parts of the molecule.

Conformational fluctuations

The calculation of the rms positional fluctuations of the backbone atoms leads to three main results. First, using time-averaged restraints, the rms fluctuations are only slightly increased with larger force constants K_{dr} (Fig. 5). In contrast, using instantaneous distance restraints, the rms positional fluctuations are much smaller, regardless of the value of the force constant. Second, the value of τ_{dr} does not affect the positional fluctuation very much, as long as it is not too short. Plots of the rms positional fluctuations for three different τ_{dr} values using the same K_{dr} value clearly demonstrate this result (Fig. 5). Whereas the atomic fluctuations in time-averaged restrained MD simulations display comparable values, the restriction of the motion of the backbone atoms by the use of instantaneous restraints is very clear from Fig. 5. These results are not only representative for the other simulations using other K_{dr} and τ_{dr} values, but they are consistent with previous work (Torda et al., 1989,1990; Pearlman and Kollman, 1991; Nanzer et al., 1994; Pearlman, 1994a). Third, the rms positional fluctuations of the backbone atoms are not well correlated with the numbers of NOEs to backbone atoms of the individual residues. It might be argued that the slightly increased rms fluctuation is due to a lack of experimental data in particular regions of the protein, but there is no evidence for this in the distribution of NOEs over the molecule (Ludvigsen et al., 1991a). Additionally, a correlation plot between the rms positional fluctuation and the number of NOEs per residue showed no correlation at all (data not shown). In fact, the distribution of the rms positional fluctuation for the backbone atoms can be related to specific secondary structures, such as the α-helix, the two β-sheets or the binding loop of CI-2, as previously reported (Nanzer et al., 1994).

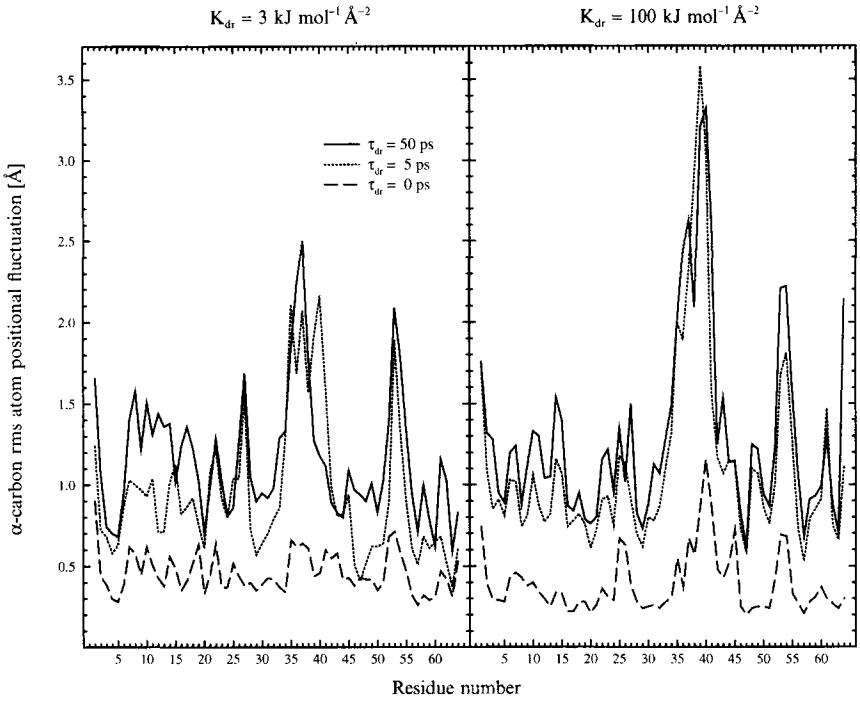

Fig. 5. Rms positional fluctuation of α-carbons of CI-2, averaged over the whole trajectory as a function of residue number. Solid line: $\tau_{dr} = 50$ ps; dotted line: $\tau_{dr} = 5$ ps; and dashed line: $\tau_{dr} = 0$ ps. Force constants are $K_{dr} = 3$ kJ mol^{-1} Å^{-2} (left panel) and 100 kJ mol^{-1} Å^{-2} (right panel).

Effect on dynamics

None of the results presented so far show much influence from the exact value of τ_{dr}, as long as τ_{dr} is not too short. On looking at the behaviour of some structural properties, however, an effect can indeed be observed. Figure 6 shows the distance between an arbitrarily chosen pair of protons as a function of time and the different panels demonstrate the effect of different values of τ_{dr}. The effect on the size of the fluctuations is not surprising. With instantaneous restraints, atomic motion is restricted, but in every case where time-averaged restraints are used, the distance varies by up to about 5 Å. The distinct time behaviour brought about by varying the value of τ_{dr} is more significant. Figure 6 suggests the presence of two

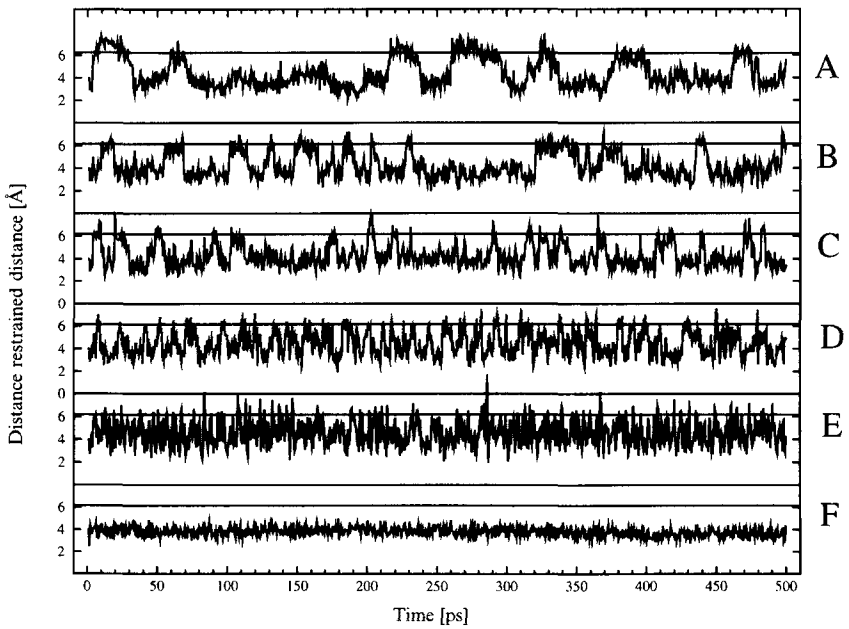

Fig. 6. Effect of τ_{dr} on dynamic behaviour. Each panel shows the distance between the amide hydrogen of Trp^{5} and the α-proton of Arg^{62}. The force constant for distance restraints was set to $K_{dr} = 30$ kJ mol^{-1} Å^{-2} in each case. The decay constant for the memory function, τ_{dr}, was set to the following values: (A) 50 ps; (B) 20 ps; (C) 10 ps; (D) 5 ps; (E) 2 ps; and (F) 0 ps. The thin line corresponds to the experimental value $r_0 = 6.2$ Å.

major states which the system visits alternately. When $\tau_{dr} = 2$ ps, the residence time in either state appears to be negligible. When $\tau_{dr} = 5$ ps, the behaviour appears almost periodic. Only for very long values of τ_{dr}, equal to 20 or 50 ps, does the system appear to move in an irregular manner. This shows that, even when average quantities such as distance violations are not affected, time-averaged distance restraining drives the system in an artificial manner. Figure 6 shows that the longer τ_{dr}, the longer the system can stay in one of its two low-energy states. This highlights the fact that τ_{dr} should ideally be chosen longer than the periods of the natural motions of the system.

Discussion and Conclusions

The major aim of this series of MD simulations was to systematically investigate the role of the two parameters that characterise time-averaged distance-restraining MD simulations. The force constant K_{dr} of the distance-restraining function determines the sum of violations and the 'largest violation'. Furthermore, K_{dr} determines the total potential energy and its fluctuation in the simulations. Ideally, one desires a minimal total potential energy and minimal violations, but Figs. 1 and 2 show a clear trade-off between low distance violations and low potential energy. The reason for this trade-off is that minima in the pseudo-energy terms and the physical force field will often not coincide, and forcing agreement with experimental data will push the system out of energetic minima.

A peculiarity of the use of time-averaged restraints is that a larger force constant K_{dr} can increase mobility. This is definitely not desirable and reflects the way the restraints can artificially drive the system. The corollary is that one should use the smallest force constant that leads to agreement with the experimental data and the longest averaging time τ_{dr}, while still aiming to have a total simulation length at least an order of magnitude longer than τ_{dr} to secure sufficient statistics.

Given the problems and artefacts associated with time-dependent distance restraints, one may ask if they should be used at all. Disturbing the time course of a simulation is not too severe a problem. The time scale of any MD simulation is somewhat artificial and an in vacuo simulation even more so. The heating of a system, however, is potentially more of a problem and may well be obscured when using coupling to a temperature bath or velocity rescaling. Clearly, one should be careful in the choice of parameters and not expect sensible results from short simulations which imply the use of a short τ_{dr}. There is another assumption implicit in this kind of simulation approach. If the system is allowed to freely roam the energy surface, it should eventually, on average, satisfy the experimental information. This relies on infinitely long simulations and a perfect force field. Neither of these conditions are fulfilled in practice.

Given these caveats, the main justifications for using time-averaged restraints may be that the artificial effects may not be too bad, that there is no other method for modelling the averaging implicit in NMR data and that modelling using static structures yields a worse representation of reality.

Acknowledgements

Financial support was obtained from the Schweizerischer Nationalfond (project 21-35909.92), which is gratefully acknowledged.

References

Berendsen, H.J.C., Postma, J.P.M., van Gunsteren, W.F., DiNola, A. and Haak, J.R. (1984) *J. Chem. Phys.*, **81**, 3684–3690.

Blundell, T.L. and Johnson, L.N. (1976) *Protein Crystallography*, Academic Press, New York, NY.

Clore, G.M., Gronenborn, A.M., Kjær, M. and Poulsen, F.M. (1987) *Protein Eng.*, **1**, 305–311.

Jardetzky, O. (1980) *Biochim. Biophys. Acta*, **621**, 227–232.

Kaptein, R., Zuiderweg, E.R.P., Scheek, R.M., Boelens, R. and van Gunsteren, W.F. (1985) *J. Mol. Biol.*, **182**, 179–182.

Ludvigsen, S., Andersen, K.V. and Poulsen, F.M. (1991a) *J. Mol. Biol.*, **217**, 731–736.

Ludvigsen, S., Shen, H., Kjær, M., Madsen, J.Chr. and Poulsen, F.M. (1991b) *J. Mol. Biol.*, **222**, 621–635.

Nanzer, A.P., Poulsen, F.M., van Gunsteren, W.F. and Torda, A.E. (1994) *Biochemistry*, **33**, 14503–14511.

Pearlman, D.A. and Kollman, P.A. (1991) *J. Mol. Biol.*, **220**, 457–479.

Pearlman, D.A. (1994a) *J. Biomol. NMR*, **4**, 1–16.

Pearlman, D.A. (1994b) *J. Biomol. NMR*, **4**, 279–299.

Ryckaert, J.-P., Ciccotti, G. and Berendsen, H.J.C. (1977) *J. Comput. Phys.*, **23**, 327–341.

Schmitz, U., Kumar, A. and James, T.L. (1992) *J. Am. Chem. Soc.*, **114**, 10654–10656.

Schmitz, U., Ulyanov, B., Kumar, A. and James, T.L. (1993) *J. Mol. Biol.*, **234**, 373–389.

Torda, A.E., Scheek, R.M. and van Gunsteren, W.F. (1989) *Chem. Phys. Lett.*, **157**, 289–294.

Torda, A.E., Scheek, R.M. and van Gunsteren, W.F. (1990) *J. Mol. Biol.*, **214**, 223–235.

Torda, A.E., Brunne, R.M., Huber, T., Kessler, H. and van Gunsteren, W.F. (1993) *J. Biomol. NMR*, **3**, 55–66.

Tropp, J. (1980) *J. Chem. Phys.*, **72**, 6035–6043.

Van Gunsteren, W.F., Kaptein, R. and Zuiderweg, E.R.P. (1984) In *Proceedings of the NATO/CECAM Workshop on Nucleic Acid Conformation and Dynamics* (Ed., Olsen, W.K.), CECAM, Orsay, pp. 79–82.

Van Gunsteren, W.F., Boelens, R., Kaptein, R., Scheek, R.M. and Zuiderweg, E.R.P. (1985) In *Molecular Dynamics and Protein Structure* (Ed., Hermans, J.), Polycrystal Book Service, Western Springs, IL, pp. 92–99.

Van Gunsteren, W.F. and Berendsen, H.J.C. (1987) *Groningen Molecular Simulation (GROMOS) library manual*, Biomos, Groningen.

Wüthrich, K., Billeter, M. and Braun, W. (1983) *J. Mol. Biol.*, **169**, 949–961.

Wüthrich, K. (1986) *NMR of Proteins and Nucleic Acids*, Wiley, New York, NY.